Med Biol Eng Comput (2008) 46:729–733
DOI 10.1007/s11517-008-0307-1

TECHNICAL NOTE

Extraction of the magnetohydrodynamic blood flow potential from the surface electrocardiogram in magnetic resonance imaging

Grace M. Nijm · Steven Swiryn · Andrew C. Larson · Alan V. Sahakian

Received: 30 July 2007 / Accepted: 16 January 2008 / Published online: 1 February 2008

Abstract The magnetohydrodynamic effect generates voltages related to blood flow, which are superimposed on the electrocardiogram (ECG) used for gating during cardiac magnetic resonance imaging (MRI). A method is presented for extracting the magnetohydrodynamic signal from the ECG. The extracted magnetohydrodynamic blood flow potential may be physiologically meaningful due to its relationship to blood flow. Removal of the magnetohydrodynamic voltages from the ECG can potentially lead to improved gating and diagnostically useful ECGs.

Keywords Magnetohydrodynamic effect · Electrocardiogram · Magnetic resonance imaging · Blood flow · Cardiac

Abbreviations

MHD	Magnetohydrodynamic
MRI	Magnetic resonance imaging
ECG	Electrocardiogram
PC	Phase contrast
GRE	Gradient echo

G. M. Nijm · S. Swiryn · A. C. Larson · A. V. Sahakian (✉)
Department of Electrical Engineering and Computer Science, Northwestern University, 2145 Sheridan Road, Evanston, IL 60208, USA
e-mail: sahakian@ece.northwestern.edu

G. M. Nijm
e-mail: g-nijm@northwestern.edu

S. Swiryn
HeartCare Midwest, Peoria, IL, USA

A. C. Larson
Department of Radiology, Northwestern University Medical School, Chicago, IL, USA

A. C. Larson · A. V. Sahakian
Department of Biomedical Engineering, Northwestern University, 2145 Sheridan Road, Evanston, IL 60208, USA

1 Introduction

The magnetohydrodynamic (MHD) potential arises when a conductive fluid such as blood travels through a magnetic field, inducing a voltage perpendicular to both the magnetic field lines and the direction of the fluid flow [2, 11]. The magnitude of this induced voltage is directly related to the magnetic flux density, fluid velocity, and inter-electrode spacing. The induced voltage V may be expressed as:

$$V = \int_0^L \boldsymbol{u} \times \boldsymbol{B} \cdot \mathrm{d}\boldsymbol{L}$$

where $\boldsymbol{u}$ is the velocity (m/s), $\boldsymbol{B}$ is the magnetic flux density (T), and $\boldsymbol{L}$ is the distance vector between electrodes (m). The MHD blood flow potential may also be expressed by a simplified equation:

$$V = BLu$$

which makes the assumption that B, L, and u are uniform and all orthogonal to one another. These equations provide a simplified method for calculating the MHD blood flow potential by assuming that flow is in a straight, cylindrical, rigid tube. Maxwell's and Navier–Stokes equations are needed to completely describe the generated MHD blood flow potentials; consequently, computational methods are typically used for such calculations.

The MHD blood flow potential is of clinical importance because it generates voltages which distort the

electrocardiogram (ECG) during cardiac MRI [10]. The MHD potential arises because of blood flow within a strong static magnetic field. It results in denigration of the diagnostic quality of the ECG, particularly for examination of the S–T segment and T wave [9], since these typically correspond to time periods of rapid ejection of blood from the ventricles, and thus, a large voltage contribution from the MHD blood flow potential. The ECG is used for gating, which coordinates the timing of MR image acquisition. Improper triggering can occur because of voltages resulting from the MHD blood flow potentials. Alternative gating methods, such as vectorcardiography and self-gating, have been proposed [1, 3, 5]. While these techniques may result in sufficiently accurate gating, they do not provide a diagnostically useful ECG during MRI since they use means other than the ECG to produce cardiac gating signals.

Since the MHD potential is related to blood flow, we hypothesized that it can be extracted from the ECG and characterized as a meaningful physiological signal on its own. Cancellation of the MHD blood flow potential can likely improve gating as well as the diagnostic quality of the ECG. As scanners evolve from 1.5T to 3.0T in clinical practice, distortion caused by the MHD blood flow potential only worsens since its magnitude is directly related to magnetic field strength. Consequently, removal of the MHD blood flow potential from the ECG is becoming increasingly more practically important.

2 Methods

The study protocol was approved by our institutional review board, and written informed consent was obtained from each subject. A Siemens 3.0T Trio MRI scanner with a wireless MR-compatible ECG lead system was used for the study. The ECG electrode pair was placed on the chest and oriented in the transverse plane in order to be orthogonal to the magnetic field lines of the static magnetic field. With this arrangement, blood flow through the aortic arch was roughly perpendicular to both the magnetic field lines and the electrode pair. The ECG electrode pair was centered on the fourth intercostal space at the left sternal border with an inter-electrode spacing of 10 cm. Thirty second ECG recordings, sampled at 100 Hz, were taken during breath holds to minimize motion artifacts due to respiration. The ECG recordings were taken with subjects in the supine and prone positions with subjects outside the magnet, inside the magnet without scanning, and inside the magnet during conventional gradient echo (GRE) scans.

MATLAB (The MathWorks Inc., Natick, MA) code was written to perform the signal processing tasks. First, baseline wander was removed by a highpass filter with a cutoff frequency of 0.5 Hz. Next, QRS complexes were detected using a modified version of the Pan and Tompkins algorithm [6] in order to identify each PQRST segment, or "beat," of the ECG signal. Template matching was applied, which involved finding the mean of beats which had at least a 95% correlation with the median beat [7]. Finally, the MHD blood flow potential was extracted by subtracting the mean beat generated when the subject was outside the magnet from the mean beat generated when the subject was inside the magnet. The MHD blood flow potential was also extracted from the subtraction of the mean beat generated with the subject outside the magnet from the mean beat generated with the subject inside the magnet during a conventional cine GRE scan. Cine GRE sequence parameters used were TR = 5.0 ms, TE = 2.6 ms, FOV = 340 mm, flip-angle = 15°, voxel size = 2.3 × 1.8 × 6.0 mm, BW = 450 Hz/pixel. GRE cine was chosen because it is a commonly used during cardiac MRI protocols [8]. The MHD blood flow potentials generated without scanning were compared with those generated while scanning.

The extracted MHD blood flow potential was analyzed as a signal, referred to as the "MHD signal." Measurements of the morphology and timing of the MHD signals included the maximum amplitude of the negative deflection of the MHD signal, the duration of the MHD negative deflection, and the delay between the onset of the QRS complex and the onset of the MHD negative deflection. A sample MHD signal indicating these measurements is shown in Fig. 1.

In addition to the ECG recordings, axial orientation 2D phase contrast (PC) MRI scans were performed

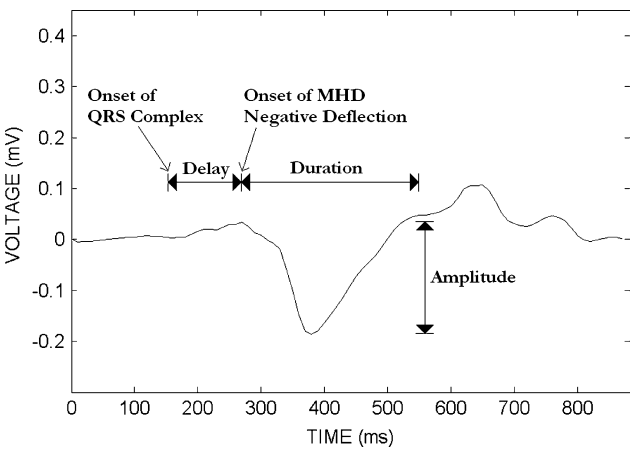

Fig. 1 Sample MHD signal with measurements of duration of the MHD negative deflection, maximum amplitude of the MHD negative deflection, and delay between onset of QRS complex and onset of the MHD negative deflection indicated. In the figure, time $t = 0$ corresponds to the P-wave onset in the original ECGs from which the MHD signal was derived

independently to allow blood flow measurements in the descending aorta near the aortic arch. These scans were performed to compare the timing of the blood flow with that observed on the MHD signal; the time resolution of the PC MRI scans was 50 ms. The sequence parameters used were TR = 66.0 ms, TE = 3.0 ms, FOV = 320 mm, flip-angle = 20°, voxel size = 2.0 × 1.3 × 5.0 mm, BW = 383 Hz/pixel, velocity encoding = 150 cm/s. Argus post-processing software was used to draw the region-of-interest within the lumen of the vessel in order to measure mean flow through the cardiac cycle.

2.1 Subject population

Data from ten healthy subjects were recorded, but the ECGs for one subject were eliminated from analysis due to poor signal quality attributed to electrode failure. Of the remaining nine subjects, three were female and six were male, ranging in age from 20 to 31 years (mean ± standard deviation, 24 ± 3 years). The subjects' average resting heart rate ranged from 46 to 76 beats per minute (bpm) (60 ± 11 bpm). The resting heart rate for each subject did not significantly change during the study.

3 Results

3.1 MHD signal characteristics

MHD signals were similar in all subjects in both the supine and prone positions and included a prominent negative deflection during the S-T segment and T wave. Figure 2 shows the MHD signals from all subjects for both the supine and prone positions. The maximum amplitude of the MHD negative deflection ranged from 0.13 to 0.27 mV (mean ± SD, 0.19 ± 0.04 mV) for the supine position compared to 0.14 to 0.30 mV (0.21 ± 0.08 mV) for the prone position. There was no statistically significant difference (NS) in amplitude between the supine and prone positions. The duration of the MHD negative deflection ranged from 320 to 380 ms (340 ± 20 ms) for the supine position compared to 300 to 360 ms (330 ± 20 ms) for the prone position (NS). The delay between the onset of the QRS complex and the onset of the MHD negative deflection ranged from 110 to 190 ms (140 ± 20 ms) for both the supine and prone positions (NS).

3.2 Effect of GRE cine scanning

The presence of GRE scanning during ECG signal acquisition had a minimal effect on the resulting MHD signals.

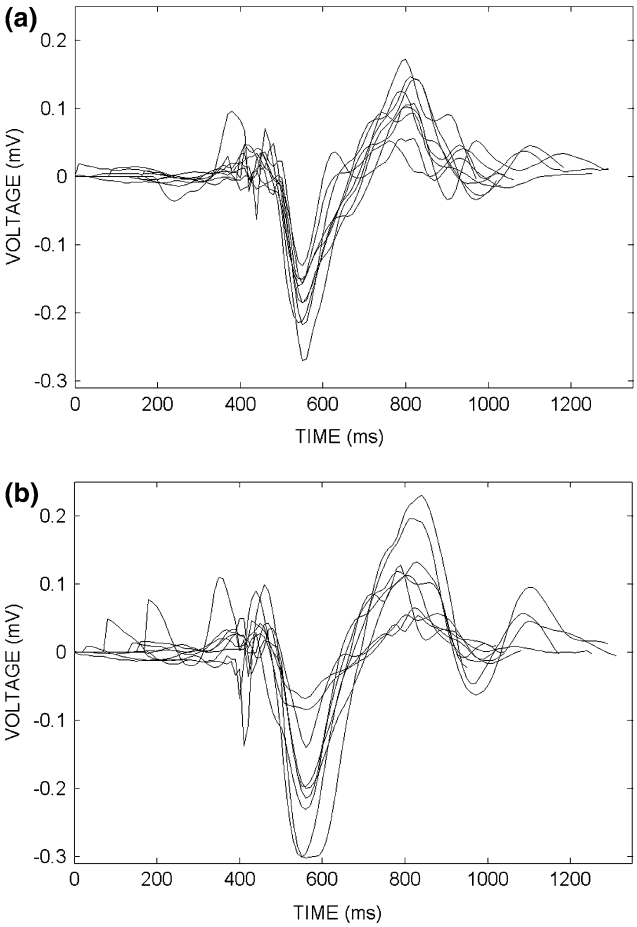

Fig. 2 MHD signals for all subjects for one cardiac cycle. **a** Subjects in the supine position, **b** Subjects in the prone position. The signals are aligned on the minimum of the primary negative deflection; they are different lengths due to different cardiac cycle lengths among the subject population

The maximum amplitude of the MHD negative deflection ranged from 0.13 to 0.28 mV (0.19 ± 0.05 mV) for the supine position and 0.13 to 0.30 mV (0.20 ± 0.06 mV) for the prone position; these values were not statistically significantly different from those obtained without scanning. Neither the duration of the MHD negative deflection nor the delay between the onset of the QRS complex and the onset of the MHD negative deflection differed from those obtained without scanning (NS). In addition, for all subjects the correlation between the two MHD signals (with and without scanning) ranged from 97.8 to 99.4%.

3.3 Comparison with MRI flow measurements

MHD signals were compared with standard MRI flow measurements in the descending aorta. The negative deflection following the QRS complex was clearly defined in both MHD and MRI flow signals for all subjects. The

duration of the MRI flow signal negative deflection ranged from 280 to 370 ms (330 ± 40 ms), which was comparable to the MHD negative deflection duration, which ranged from 320 to 380 ms (340 ± 20 ms) for the supine position and 300 to 360 ms (330 ± 20 ms) for the prone position (NS). The minimum of the MRI flow signal lagged behind the minimum of the MHD signal in all subjects; the difference in timing between the minima of these signals ranged from 20 to 90 ms (60 ± 20 ms) for the supine position and 10 to 80 ms (50 ± 20 ms) for the prone position (NS). The MHD signals and MRI flow data for a sample subject are shown in Fig. 3.

4 Discussion

The main finding of this work was that the MHD blood flow potential can be extracted from the ECG obtained in the MRI magnet. In theory, the MHD blood flow potential should reflect the net effect of the blood flow occurring at a particular instant and orientation, as registered on the surface of the body. A primary contributor to the MHD blood flow potential observed in this study was likely blood flow in the aortic arch for several reasons. First, the velocity of blood is greatest in the aorta immediately following ejection from the left ventricle. Second, the aorta is the largest diameter blood vessel. Finally, blood flow through the aortic arch is approximately perpendicular to both the electrode pair used in this study and the magnetic field lines of the MRI magnet. The magnitude of the MHD blood flow potential is influenced by the velocity of the fluid and the orientation of flow relative to the electrode pair and the magnetic field lines. Though blood flow in other vessels which are orthogonal to the magnetic field lines and the electrode pair may also contribute to the magnitude of the MHD blood flow potential, the velocity of blood flow is greatest in the aorta; therefore, due to its orientation, flow in the aortic arch should make the most significant contribution to the observed MHD blood flow potential. Since the aortic arch is roughly orthogonal to the magnetic field lines and the electrode pair in both the supine and prone positions, the MHD signals were, as expected, not significantly different when subjects were supine or prone. The observed delay between the onset of the QRS complex and the onset of the MHD deflection agreed with the anticipated lag as a result of the delay between electrical activation and mechanical activation, time for isovolumetric contraction prior to ejection, and time for the flow to propagate into the aortic arch [4].

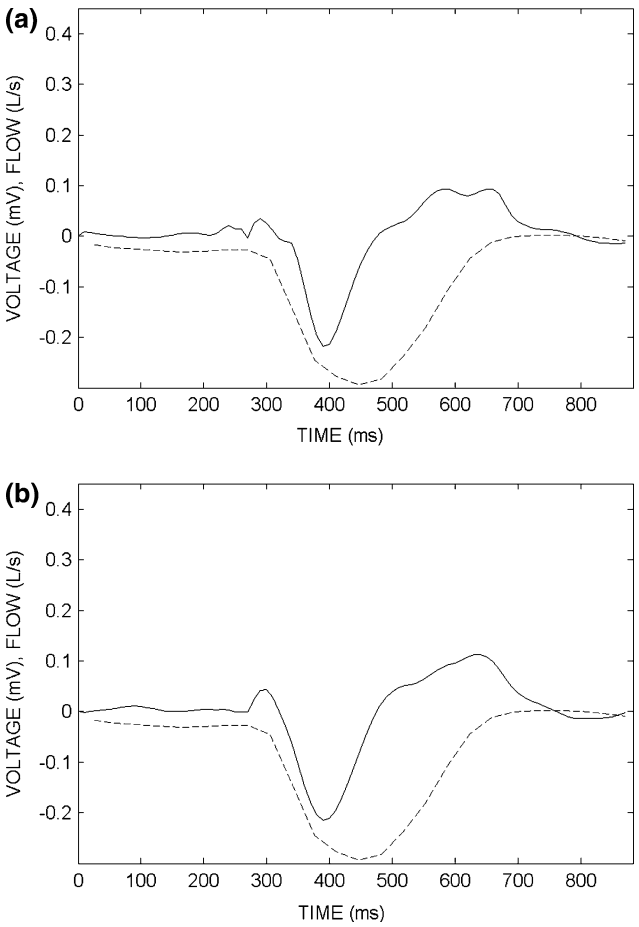

Fig. 3 MHD signal (*solid line*) and MRI flow (*dashed line*). **a** Subject in the supine position, **b** Subject in the prone position

Scanning during ECG signal acquisition had a minimal effect on the resulting MHD signal. This is reasonable because radiofrequency interference was removed by filtering, and an optimized lead system as well as the use of template matching minimized the switching MR gradient artifacts.

The correlation in timing and similarity in morphology between the independently obtained MRI flow data and the MHD signal help to verify that the MHD signal is in fact flow-related. The coarse time resolution of 50 ms for the MRI flow data may explain the small discordance in timing between the two signals. Although MRI flow measurements were used for sake of comparison in this study, a major potential advantage of flow data obtained from the ECG is its superior temporal resolution in comparison to MRI flow data. In this study, the ECG was sampled at 100 Hz while MRI flow measurements were acquired only every 50 ms, or at a rate of 20 Hz. In addition, the negative deflection of the MHD signal begins after and ends before the negative deflection of the MRI flow signal because the MHD signal is generated over a shorter time interval than the MRI flow signal. Blood flow through the aortic arch largely produces the negative deflection of the MHD signal; however, the negative deflection of the MRI flow signal is produced before flow has propagated into the

aortic arch and continues after the bolus of blood has traveled through the aortic arch.

The next set of challenges will be to use these methods not only to improve gating but also to record a diagnostic quality ECG during cardiac MRI. Further application of this work has potential to make use of the MHD signal as a physiologically meaningful signal due to its relationship to blood flow.

5 Conclusions

The MHD signal can be extracted from the ECG obtained in the MRI magnet. The MHD signal so obtained correlates well in timing with the flow signal acquired from standard MRI flow measurement techniques.

Acknowledgments This material is based upon work supported under a National Science Foundation Graduate Research Fellowship, NIH HL079148, and a grant from the Dr. Scholl Foundation.

References

1. Crowe ME, Larson AC, Zhang Q, Carr J, White RD, Li D, Simonetti OP (2004) Automated rectilinear self-gated cardiac cine imaging. Magn Reson Med 52:782–788
2. Dimick RN, Hedlund LW, Herfkens RJ, Fram EK, Utz J (1987) Optimizing electrocardiograph electrode placement for cardiac-gated magnetic resonance imaging. Invest Radiol 22:17–22
3. Fischer SE, Wickline SA, Lorenz CH (1999) Novel real-time R-wave detection algorithm based on the vectorcardiogram for accurate gated magnetic resonance acquisitions. Magn Reson Med 42:361–370
4. Guyton AC, Hall JE (2000) Textbook of medical physiology, 10th edn. W.B. Saunders, Philadelphia
5. Larson AC, White RD, Laub G, McVeigh ER, Li D, Simonetti OP (2004) Self-gated cardiac cine MRI. Magn Reson Med 51:93–102
6. Pan J, Tompkins WJ (1985) A real-time QRS detection algorithm. IEEE Trans Biomed Eng 32:230–236
7. Slocum J, Byrom E, McCarthy L, Sahakian AV, Swiryn S (1985) Computer-detection of atrioventricular dissociation from surface electrocardiograms during wide QRS complex tachycardias. Circulation 72:1028–1036
8. Sola S, White RD, Desai M (2006) MRI of the heart: Promises fulfilled? Cleve Clin J Med 73:663–670
9. Tenforde TS, Gaffey CT, Moyer BR, Budinger TF (1983) Cardiovascular alterations in Macaca monkeys exposed to stationary magnetic fields: experimental observations and theoretical analysis. Bioelectromag 4:1–9
10. Tenforde TS (2005) Magnetically induced electric fields and currents in the circulatory system. Prog Biophys Mol Biol 87:279–288
11. Togawa T, Okai O, Oshima M (1967) Observation of blood flow e.m.f. in externally applied strong magnetic field by surface electrodes. Med Biol Eng 5:169–170